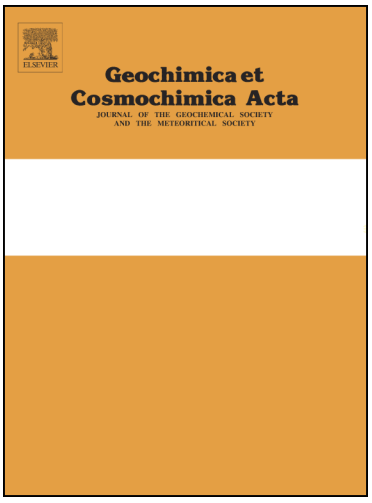

Differential metamorphic effects on nitrogen isotopes in kerogen extracts and bulk rocks

Eva E. Stüeken, Jon Zaloumis, Jana Meixnerová, Roger Buick

PII: S0016-7037(17)30500-8
DOI: http://dx.doi.org/10.1016/j.gca.2017.08.019
Reference: GCA 10424

To appear in: *Geochimica et Cosmochimica Acta*

Received Date: 15 April 2017
Accepted Date: 9 August 2017

Please cite this article as: Stüeken, E.E., Zaloumis, J., Meixnerová, J., Buick, R., Differential metamorphic effects on nitrogen isotopes in kerogen extracts and bulk rocks, *Geochimica et Cosmochimica Acta* (2017), doi: http://dx.doi.org/10.1016/j.gca.2017.08.019

Differential metamorphic effects on nitrogen isotopes in kerogen extracts and bulk rocks

Eva E. Stüeken[1,2,4]*, Jon Zaloumis[3,4], Jana Meixnerová[2,4], Roger Buick[2,4]

1. present address: University of St Andrews, School of Earth & Environmental Sciences, St Andrews, Fife, KY16 9AL, Scotland, UK
2. NASA Astrobiology Institute, Virtual Planetary Laboratory, Seattle, Washington 98195, USA
3. present address: Arizona State University, School of Earth and Space Exploration, Tempe AZ 85281, USA
4. University of Washington, Department of Earth & Space Sciences and Astrobiology Program, Seattle WA 98195-1310, USA
* corresponding author ees4@st-andrews.ac.uk

Abstract

The last decade has seen a steady rise in the number of publications on nitrogen isotopes in sedimentary rocks, which have become an established tool for investigating the evolution of life and environmental conditions. Nitrogen is contained in sedimentary rocks in two different phases: bound to kerogen or substituted in potassic minerals (mostly K-bearing phyllosilicates and feldspars). Isotopic measurements and interpretations typically focus either on kerogen extracts alone or on bulk rocks that include both phases. The community is split about which sample type more accurately captures the original composition of the biomass. To address this question, we combined nitrogen isotopes and carbon-to-nitrogen ratios with carbon-to-hydrogen ratios which act as an independent proxy for metamorphic alteration. Our results reveal that metamorphism drives kerogen-bound nitrogen isotopically lighter while silicate-bound nitrogen becomes heavier. For rocks up to greenschist facies, the isotopic effect of this internal partitioning (up to 3-4‰) is larger than the isotopic effect of metamorphic nitrogen loss from the system (up to 1-2‰). The opposite may be true for higher metamorphic grades. We conclude that for low-grade sedimentary rocks with more than 60% of their total nitrogen residing in the silicate phase the primary isotopic composition of the biomass is best approximated by the bulk rock measurement, whereas for high-grade rocks the kerogen extract may be the more accurate proxy. The isotopic difference between nitrogen phases can thus serve as a rough indicator of the degree of metamorphic alteration.

1. Introduction

Nitrogen isotopes have become a widely used tool for reconstructing the evolution of the global biogeochemical nitrogen cycle (Ader et al., 2016; Algeo et al., 2014; Pinti and Hashizume, 2011b; Stüeken et al., 2016; Thomazo et al., 2009), the origin and expansion of key nitrogen metabolisms (Beaumont and Robert, 1999; Garvin et al., 2009; Godfrey and Falkowski, 2009; Stüeken et al., 2015a), and the redox structure and alkalinity of ancient water bodies (Ader et al., 2014; Busigny et al., 2013; Godfrey et al., 2013; Koehler et al., 2017; Kump et al., 2011; Papineau et al., 2009; Pinti and Hashizume, 2001; Pinti et al., 2001; Stüeken, 2013; Stüeken et al., 2015b; Talbot and Johannessen, 1992; Zerkle et al., 2017). Most studies typically target sedimentary rocks that are rich in organic matter. Almost all nitrogen in such rocks was originally captured by living organisms that either fixed N_2 or assimilated dissolved NO_3^-, NH_3 or NH_4^+ with a characteristic isotopic composition. As these organisms died and settled to the seafloor, their isotopic composition was archived in the sedimentary record. Initially, this nitrogen is thus all organic-bound. However, through biomass degradation in sediments during diagenesis, ammonium is liberated into pore waters where it can reach mM concentrations (e.g. Boudreau and Canfield, 1988; Müller, 1977; Rosenfeld, 1979). This biogenic ammonium can adsorb onto clay minerals and get incorporated into their crystal lattice, substituting for K^+ (Honma and Itihara, 1981; Itihara and Honma, 1979; Schroeder and McLain, 1998). During metamorphism, nitrogen is progressively lost from both the kerogen and the silicate phases as either N_2 or NH_3, depending on redox and pH conditions. Several studies of bulk rocks have documented an increase of C/N ratios and $\delta^{15}N$ values with increasing metamorphic grade (Bauersachs et al., 2009; Bebout et al., 1999; Bebout and Fogel, 1992; Boyd and Phillippot, 1998; Haendel et al., 1986; Jia, 2006; Mingram and Bräuer, 2001; Palya et al., 2011; Pinti et al., 2009), although to varying degrees and not under all circumstances (Ader et al., 2006; Busigny et al., 2003; Plessen et al., 2010; Yui et al., 2009). In most cases, the net isotopic effect is on the order of 1-2 ‰ up to greenschist facies, but is often larger at higher metamorphic grades (Thomazo and Papineau, 2013). Boudou et al. (2008) suggested that metamorphic nitrogen loss is mediated by hot fluids. Furthermore, it has been hypothesized that nitrogen could be added to the metamorphic system by metasomatic fluids (e.g. Kump et al., 2011; Schimmelmann et al.,

2009) which could have picked up ammonium from magmatic sources (van Zuilen et al., 2005) or from other sedimentary rocks (Svensen et al., 2008).

These diagenetic and metamorphic processes have led to a disagreement in the literature about which nitrogen phase most accurately captures the original isotopic composition of the biomass. Some studies measure bulk sedimentary rocks, arguing that the combination of kerogen and silicate-bound nitrogen represents a larger fraction of the total initial nitrogen pool (Ader et al., 2014; Busigny et al., 2011; Godfrey et al., 2013; Koehler et al., 2017; Stüeken, 2013; Stüeken et al., 2015a; Thomazo et al., 2011). Others prefer to rely on the kerogen phase only, because it represents the actual biomass residue and is supposedly less easily altered during metasomatism (Godfrey and Falkowski, 2009; Kump et al., 2011; although see Schimmelmann and Lis, 2010, for an alternative view). However, no single study has so far provided quantitative evidence for either position. As recently reviewed by Ader *et al.* (2016) and shown in Fig. 1, kerogen-bound nitrogen is in most cases isotopically lighter than bulk rocks by a few permil (Ader et al., 2014; Godfrey and Falkowski, 2009; Godfrey et al., 2013; Kump et al., 2011; Stüeken et al., 2015a, this study; Yamaguchi, 2002; Zerkle et al., 2017). This offset is unlikely to be due to a biological process if the transfer of ammonium from biomass to clay minerals happens during late diagenesis (Schroeder and McLain, 1998). Instead, it could be due to the preferential removal of isotopically heavy proteins (Altabet et al., 1991; Macko et al., 1987), or preferential preservation of isotopically light porphyrins such as bacteriochlorophyll (Beaumont et al., 2000; Chicarelli et al., 1993; Kashiyama et al., 2008). In both cases, clay minerals would incorporate isotopically heavy nitrogen, as observed. However, some studies found no systematic offset between the kerogenous and bulk phases (Bauersachs et al., 2009; Koehler et al., 2017), while Godfrey et al. (2013) reported unusually large offsets of up to 13‰ in samples affected by contact metamorphism. These observations suggest that the isotopic difference between the two phases cannot be purely controlled by a universal diagenetic process such as protein degradation or porphyrin preservation. Additional post-diagenetic processes must play a role and demand investigation to settle the debate over which nitrogen phase best captures primary metabolic signatures.

To address this question, we combined nitrogen isotope data and C/N ratios from bulk rocks and kerogen isolates with carbon-to-hydrogen ratios (C/H) of kerogen. C/H ratios are a long-established proxy for metamorphic alteration of biomass, because H is lost preferentially to

C, even at sub-greenschist metamorphic grades (Hayes et al., 1983; Van Krevelen, 1950; Van Krevelen, 1984). In the context of our study, C/H ratios are the preferred proxy for metamorphic alteration, because (1) they directly assess alteration of organic matter, which is the original source of nitrogen in sedimentary rocks, (2) they change continuously rather than in steps, unlike metamorphic mineral assemblages, and (3) they are sensitive to metamorphic alteration across the entire range of interest from diagenesis up to amphibolite facies, unlike other organic indices such as biomarker maturity parameters and vitrinite reflectance or mineralogical measures such as illite crystallinity and chlorite geothermometry. We apply this approach to a set of samples spanning the Mesoarchean to the Permian in age (Table 1). This sample set covers a wide range of metamorphic grades from nearly unmetamorphosed to upper greenschist/lower amphibolite facies, which allows us to reconstruct large-scale and general metamorphic effects on the nitrogen isotope data.

2. Methods

Some of the carbon and nitrogen data used in this study were previously published (Table 1). To expand this data-set, we added new bulk rock measurements, performed kerogen extractions and obtained C/H ratios for all our kerogen isolates. Newly added samples come from the Paleoarchean Duffer Formation (drill core ABDP-2, e.g. Wille et al., 2013), the Neoarchean Jeerinah Formation (drill core WRL-1, e.g. Eigenbrode and Freeman, 2006), the Permian Sulphur Mountain Formation (outcrop samples 50.675171°N, 115.080011°W, Schoepfer et al., 2012; Stüeken et al., 2015c) and the Neoproterozoic Callanna Group (outcrop samples 29.724612°S, 137.979923°E and 31.898134°S, 138.633467°E, e.g. Preiss, 1987).

2.1. Sample preparation

Sample preparation followed established protocols (Koehler et al., 2017; Stüeken, 2013; Stüeken et al., 2015a). The outer surfaces of hand samples (both outcrop and drill core) were trimmed with a rock saw. The rocks were then fragmented into sub-cm pieces, transferred into a baked glass beaker (500°C overnight), and rinsed with water (DI, 18MΩ), HCl (2N, reagent grade), water, alcohol (concentrated, reagent grade), and again water. The clean rock chips were

dried overnight at 60°C in a closed oven, and then pulverized with an Al_2O_3 ceramic puck mill. The mill was cleaned with baked sand (1100°C overnight), DI-water and alcohol after every sample. Powders were transferred into baked scintillation vials (500°C overnight) via an alcohol-rinsed plastic weigh boat.

For bulk rock analyses, 0.5 g of rock powder were treated with 6N HCl (reagent grade) to remove carbonate. The powder was weighed into baked glass centrifuge tubes (500°C), mixed with ~10ml of HCl with a glass stirring rod, sonicated for about 10 minutes, and left to react at 60°C overnight. The acid was replaced three times to ensure complete dissolution of sparingly soluble carbonate phases. The samples were then centrifuged, the acid was decanted and the powder was washed three times with DI-H_2O to remove any excess chloride that may otherwise corrode the sample holders or the elemental analyzer.

Kerogen isolates were prepared using a modified protocol from Robl & David (1993) as in previous studies (Stüeken et al., 2015a; Stüeken et al., 2015b). Approximately 5g of rock powder were weighed into a 250ml Nalgene bottle and mixed with 100ml of 6N HCl to remove carbonate. The bottles were placed into a shaking water bath at 50°C overnight. The following day, the bottles were centrifuged and the HCl was decanted. The powder was rinsed once with DI-H_2O. Silicates were then dissolved with a mixture of 100ml of DI-water and 100ml of concentrated HF (reagent grade) in the shaking water bath at 50°C overnight. The HF was decanted after centrifugation. Secondary fluoride precipitates were removed with 200ml of BF_3, which was prepared from 62.5g of boric acid powder (reagent grade), 100ml of HF and 100ml of DI-H_2O. The samples with BF_3 solution were placed into the shaking water bath overnight at 50°C and centrifuged the next day to decant the solution. The samples were then washed 3-4 times with hot DI-H_2O and sonicated between washes to remove any residual boric acid and HF. The resulting kerogen extract was poured into a baked scintillation vial with ~10ml of DI-H_2O and placed into a freeze-drier for two days until it was completely dry. A glass rod was used to re-homogenize the extracted kerogen.

2.2. Isotopic analyses and C/N ratios

Analyses were carried out with a Costech elemental analyser coupled to a MAT253 continuous flow IRMS via a Conflo III interface, following established protocols in the

University of Washington Isolab (Koehler et al., 2017; Stüeken, 2013; Stüeken et al., 2015a). For bulk rocks ($\delta^{15}N_{bulk}$), 20-100mg of decarbonated powder were weighed into a tin capsule and then flash-combusted with 20ml of O_2 (1bar). All analyses were followed by a blank. Background levels of N_2 contained in the O_2 gas were monitored with the blanks, and the sample data were corrected by mass balance. The $^{15}N/^{14}N$ raw data were calibrated with the two-point method (Coplen et al., 2006) relative to the air reference value (Mariotti, 1983) with well-characterized in-house standards of glutamic acid and dried salmon, which range from -5.7‰ to +11.3‰ in $\delta^{15}N$ and thus bracket nearly all our samples (only two data points were as heavy as +13‰). Carbon and nitrogen quantities were determined from the peak area, calibrated with known quantities of N_2 and CO_2 from a series of the glutamic acid standard. Long-term reproducibility as monitored with our UW-McRae in-house rock standard was 0.3‰ (1 standard deviation, SD) for $\delta^{15}N$, 4% (relative error, RE) for N content, 2% for total organic carbon (TOC) content (RE) and 4% for C/N ratios (RE). Results are expressed in standard delta notation (Equation 1):

$$\delta^{15}N\ [‰] = (^{15}N/^{14}N)_{sample}/(^{15}N/^{14}N)_{air} - 1 \quad (1)$$

Measurements of kerogen extracts ($\delta^{15}N_{kerogen}$) followed the same protocol with the only difference being that N_2 and CO_2 were analyzed separately. In the first run, 0.5mg of material was weighed out to determine the organic carbon content and approximate nitrogen content of the extract. For the second run, the mass was then optimized for a strong N_2 signal (typically a few mg for a minimum of 5x above blank levels), which usually resulted in excess amounts of CO_2 that would have saturated the detectors. To avoid saturation, the CO_2 was scrubbed from the gas stream with soda lime. The isotopic reproducibility of the kerogen extraction was 0.1‰ for $\delta^{15}N$ as determined with the in-house rock standard UW-McRae. As shown in previous studies with the same analytical protocol using the same equipment (Stüeken et al., 2015a), we did not encounter any problems with incomplete combustion, which we attribute to the large quantity of O_2 (20ml) used in the EA (Han et al., 2017), the large tin capsules (9 x 5 mm) that increase the flash combustion temperature to 1700°C (Kirsten and Hesselius, 1983; Therion et al., 1986), and the biweekly replacement of the reagent columns. The fractions of kerogen and silicate phases

($f_{kerogen}$ and $f_{silicate}$) and the isotopic composition of the silicate-bound nitrogen phase ($\delta^{15}N_{silicate}$) were calculated by mass balance (Equations 2 and 3):

$$f_{kerogen} = 1 - f_{silicate} = (N\ [wt\%] / C\ [wt\%])_{kerogen} \cdot (TOC\ [wt\%] / TN\ [wt\%])_{bulk} \quad (2)$$

$$\delta^{15}N_{silicate} = (\delta^{15}N_{bulk} - (f_{kerogen} \cdot \delta^{15}N_{kerogen})) / f_{silicate} \quad (3)$$

The calculated isotopic difference between kerogen- and silicate-bound nitrogen is defined here as $\Delta^{15}N$ (Equation 4):

$$\Delta^{15}N = \delta^{15}N_{kerogen} - \delta^{15}N_{silicate} \quad (4)$$

Molar C/N ratios, which are commonly used in the literature, were calculated from mass ratios by multiplication with molar masses of 14.01 g/mol for nitrogen and 12.01 g/mol for carbon.

2.3. Organic C/H ratios of kerogen isolates

For analyses of C/H ratios, an aliquot of each kerogen extract was sent to the Marine Science Institute Analytical Lab at the University of California, Santa Barbara. The measurements were made in an automated organic elemental analyzer (CEC 440HA) with high-precision thermal conductivity detectors. The reproducibility of C/H ratios determined with kerogen separates of our UW-McRae rock standard was 1% (relative error, RE).

2.4. Potassium abundances in bulk rocks as a proxy for metasomatism

Following Kump et al. (2011), we obtained measurements of K abundances for a subset of our samples to track the effects of metasomatic alteration on the nitrogen isotope data. K is mobile in sediments because it can be released from K-feldspars during diagenesis (van de Kamp, 2016). The similarity in charge and size between K^+ and NH_4^+ has led to the proposal that NH_4^+ may follow K^+ in metasomatic fluids (Godfrey and Falkowski, 2009; Kump et al., 2011). We adopt this approach of tracking metasomatic alteration with K, but we note that a correlation between K and nitrogen isotopes or abundances may also reflect preferential retention of

biogenic NH_4^+ in illite-rich sediments (Palya et al., 2011; Schroeder and McLain, 1998) rather than external addition of NH_4^+ from foreign sources. To obtain K measurements, we submitted sample powders to ALS Geochemistry, where they were dissolved with HF, HNO_3, $HClO_4$ and HCl and analyzed by ICP-MS.

3. Results

C/H ratios in our kerogen extracts range from 0.83 to 17.18 (H/C = 1.20 to 0.06) (Fig. 2, Table 1). The logarithm of C/H ratios covaries with the logarithm of C/N ratios of both kerogen (r^2 = 0.67) and bulk rocks (r^2 = 0.50) (Fig. 2), reflecting preferential nitrogen loss relative to carbon with increasing metamorphic grade, as expected (Hayes et al., 1983). C/N ratios of bulk rocks are consistently lower than C/N ratios of kerogen (Fig. 2), because the bulk rock measurements include the silicate-bound nitrogen phase, which in the absence of silicate-bound carbon creates a dilution effect.

For most samples, the kerogen isolate is isotopically lighter than the bulk value and the calculated silicate fraction. The isotopic difference between kerogen- and silicate-bound nitrogen ($\Delta^{15}N$) negatively covaries with log(C/H) (r^2 = 0.56, Fig. 3), *i.e.* the difference becomes larger with higher metamorphic grade. The fraction of kerogen-bound nitrogen ($f_{kerogen}$) is not correlated with log(C/H) (r^2 = 0.01, Fig 4A) nor with $\Delta^{15}N$ (r^2 = 0.03, Fig. 4B). We also found no correlation between $\Delta^{15}N$ and total K content (Fig. 5), with the exception of the Callanna Group.

4. Discussion

4.1. Quality of kerogen extracts

Ader et al. (2006) showed that the quality of kerogen isolates and thus the isotopic data obtained from them can be compromised if secondary fluorides are retained during the kerogen extraction. However, it is unlikely that the observed trends in our data are affected by this issue for several reasons. First, our kerogen extraction method, adopted from Robl & Davis (1993), involves a BF_3 step, which specifically dissolves fluoride phases and which was not part of some previous protocols (Ader et al., 2006; Durand and Nicaise, 1980). Second, we observe no

significant correlation between the carbon content of the kerogen isolates and $\Delta^{15}N$. The correlation coefficient r^2 equals 0.32 if all points are included, but it drops to 0.06 after excluding the four most extreme data points, which makes this trend very weak (Fig. 6). The carbon content of kerogens ranges from 0.7 to 93.2% (average 43.6 ± 22.0%) which probably reflects dilution by common recalcitrant minerals in the original rock that are only weakly soluble in concentrated HF at 50°C (e.g. pyrite, pyrophyllite, zircon, rutile, chromite, garnet, barite, some phosphate minerals, see Durand and Nicaise, 1980; Hoops, 1964) rather than by secondary fluorides. For example, the Sulphur Mountain samples, which are lowest in TOC, reportedly have high phosphate, barium and pyrite levels (Schoepfer et al., 2013; Schoepfer et al., 2012), which may explain the low purity of the kerogen isolates. Lastly, the metamorphic grades inferred from our measured C/H ratios are consistent with metamorphic facies based on mineralogical indicators – if present. The C/H ratios range from 0.83 to 17.18. For reference, fresh bacterial biomass has a C/H ratio of 0.63 (H/C ~ 1.6). Hayes et al. (1983), who calibrated C/H ratios against mineralogically defined metamorphic zones, showed that C/H ratios increase to ~2 in prehnite-pumpellyite facies, ~5 in lowermost greenschist facies, ~10 in upper greenschist facies and higher values in amphibolite facies. For example, in the Belt Supergroup, we measured C/H ratios of 3.1 ± 0.7, consistent with the prehnite-pumpellyite metamorphic grade inferred from the mineralogy (Schieber, 1989). For the Roper Group, we measured C/H = 1.2 ± 0.3, consistent with previous evidence that these rocks have not been metamorphosed beyond the oil window (Jackson et al., 1988). And our C/H ratios of 7.9 ± 0.5 for the Jeerinah Formation agree with recent RockEval evidence for metamorphic alteration to lower greenschist facies (French et al., 2015).

Our samples thus span a wide metamorphic range, which allows us to discern first-order metamorphic trends on the isotopic data. The strong correlation between C/H and C/N ratios (Fig. 2) is evidence that the relative abundance of nitrogen in these samples is to first order controlled by metamorphic alteration. The correlation is slightly weaker for bulk C/N than for kerogen isolates (Fig. 2), which is most likely an artifact of mixing between organic and inorganic nitrogen phases that may respond somewhat differently to metamorphic N-loss. However, to first order, the similarity in the two trend lines indicates that bulk rocks and kerogen isolates behave similarly. This further suggests that our overall data are unlikely to be affected by metasomatic addition of nitrogen. This does not rule out potential metasomatic overprinting for

individual subsets of our samples (e.g. the Callanna Group where $\Delta^{15}N$ and total K are correlated, Fig. 5), but such small-scale effects do not invalidate our interpretation of large-scale metamorphic trends in the isotopic data across this diverse suite of samples.

4.2. Isotopic separation between nitrogen phases

The anti-correlation between $\Delta^{15}N$ and log(C/H) (Fig. 3) shows that the first-order trend with increasing metamorphic grade is the result of an isotopic separation between the kerogen-bound and silicate-bound nitrogen phases. This finding is consistent with data from the Paleoproterozoic Animikie basin where kerogen isolates are most negative and offset from bulk values in those samples that have been most affected by contact metamorphism (Godfrey et al., 2013). However, as indicated by the lack of correlation with $f_{kerogen}$ (Fig. 4), this separation is not related to the degree of nitrogen transfer from organic matter to phyllosilicate minerals. To further investigate the cause of this isotopic separation we plotted $\Delta^{15}N$ against the individual isotopic composition of each of the phases $\delta^{15}N_{kerogen}$ and $\delta^{15}N_{silicate}$. As shown in Fig. 7, both phases vary substantially and no trends are discernable if all data points are plotted. However, some of this variability may result from differences in the original isotopic composition of the biomass caused by differing metabolic strategies or redox conditions of the ocean during the time of deposition (reviewed by Ader et al., 2016; Stüeken et al., 2016).

To isolate possible metamorphic trends, it is important to select samples that reflect the same environmental and metabolic regime. In Fig. 8 we plotted only those samples for which both $\delta^{15}N_{kerogen}$ and $\delta^{15}N_{bulk}$ fall between -2‰ and +1‰, which is the canonical range of biological N_2 fixation by Mo-nitrogenase and would be interpreted as such regardless of whether the interpretation is based on kerogen isolates or bulk rocks (e.g. Garvin et al., 2009; Godfrey and Falkowski, 2009; Stüeken et al., 2015a; Zerkle et al., 2017). The isotopic effect of biological N_2 fixation usually dominates sedimentary nitrogen isotope signals in settings that are depleted in dissolved NH_4^+ and NO_3^-. During the Precambrian, this appears to have been the case during episodes of widespread ocean anoxia (Ader et al., 2016; Stüeken et al., 2016; Thomazo et al., 2009). Hence this subset of samples should not have been significantly affected by redox reprocessing. As shown in Fig. 8A, we find that within these samples the silicate-bound nitrogen tends to become heavier while kerogen-bound nitrogen becomes lighter as $\Delta^{15}N$ gets more

negative. This observation becomes clearer when we focus on individual geological units. Samples from the Soanesville Group (Fig. 8C, 7D) show the same trend with an isotopic offset of 3-4‰ between the two nitrogen phases. Importantly, the Soanesville Group does not show a correlation between K and $\Delta^{15}N$ (Fig. 5), which rules out metasomatic alteration as the cause of this trend. A smaller set of samples from the Belt Supergroup possibly shows similar trends in $\delta^{15}N_{kerogen}$ and $\delta^{15}N_{silicate}$, though smaller in magnitude (0.5-2‰) (Fig. 8B). These observations show that the widening of the isotopic difference between the two phases ($\Delta^{15}N$) appears to be driven not just by one phase but by both at the same time. Kerogen becomes isotopically lighter while silicates become heavier.

The cause of this internal partitioning cannot be directly inferred from our data, but it is perhaps most parsimoniously explained by equilibrium fractionation between the organic and inorganic nitrogen phases. It is unlikely to be a kinetic effect, because kinetic isotope fractionation is usually associated with unidirectional transformations, such as redox reactions or volatilization. If kinetic effects were driving the observed phase partitioning, then we would expect a progressive increase or decrease in $f_{kerogen}$ with metamorphic grade – counter to what is observed. Instead, an equilibrium process is most likely and consistent with changing bonding environments of nitrogen in the two phases. As shown by Boudou et al. (2008), who investigated the bonding environment of organic nitrogen during metamorphism, nitrogen-bearing functional groups are progressively transformed into aromatic heterocyclic structures. Similarly, the bonding environment of silicate-bound nitrogen may change as silicate minerals undergo metamorphic reactions, including dewatering of clay minerals and crystallization of micas (see also Pinti et al., 2009). It is therefore conceivable that isotopic re-equilibration occurs within assemblages of organic matter and silicate minerals. The equilibration itself may be driven by hot fluids, possibly derived from dewatering minerals, as proposed for alteration of organic nitrogen (Ader et al., 2006; Boudou et al., 2008).

4.3. Internal fractionation versus nitrogen loss

To further explore the mechanism behind this process, we used an equilibrium fractionation model to reconstruct the trends in our data (Fig. 9). Initially, almost all nitrogen would be biomass-bound, corresponding to $f_{kerogen} \approx 100\%$ in this model. Transfer of nitrogen

into silicate minerals likely occurs during diagenesis, when NH_4^+ concentrations in pore waters are high due to the degradation of organic matter (Boudreau and Canfield, 1988; Rosenfeld, 1979). At this pre-metamorphic stage, the isotopic fractionation between the two phases is likely small (Bauersachs et al., 2009) or even opposite to metamorphosed samples, as indicated by our data points with low C/H ratios (Fig. 3). In Fig. 9A, we assume a diagenetic effect of 0‰, which means that an unmetamorphosed sample moves along the x-axis to a specific value of $f_{kerogen}$ (e.g. light blue circle), but the kerogen- and silicate-bound nitrogen phases remain isotopically identical. The exact value $f_{kerogen}$ may depend on the mineralogy, porosity and permeability of the rock as well as the degree to which kerogen is adsorbed to clay minerals (Hedges and Keil, 1995; Müller, 1977).

We now consider two metamorphic effects: (type 1) internal isotopic partitioning between kerogen and silicates, and (type 2) loss of nitrogen from the system with a preference for ^{14}N. As suggested by our data in Fig. 8, internal partitioning (type 1) forces kerogen-bound nitrogen lighter (green arrow in Fig. 9A) and silicate-bound nitrogen heavier (brown arrow in Fig. 9A). Where $f_{kerogen}$ is large, the net effect on $\delta^{15}N_{kerogen}$ is likely smaller then in cases where $f_{kerogen}$ is small, because large reservoirs are generally more difficult to perturb isotopically. As discussed above. the isotopic partitioning between the kerogen and silicate phases most likely follows an equilibrium fractionation pathway with a small fractionation (shallow slope in Fig. 9A) at very low metamorphic grade and a larger fractionation (steeper slope in Fig. 9A) with increasing metamorphic grade. For example, our Soanesville data show a fractionation between the two nitrogen phases of 3-4‰ at lower greenschist facies (H/C ~ 0.15), whereas the Belt Supergroup data show a fractionation of 0.5-2‰ at prehnite-pumpellyite facies (H/C ~ 0.33). We define this internal fractionation as $\varepsilon_{internal}$ (Equation 5):

$$\varepsilon_{internal} = 1000 \cdot ((^{15}N/^{14}N)_{kerogen} / (^{15}N/^{14}N)_{silicate} - 1) \approx \delta^{15}N_{kerogen} - \delta^{15}N_{silicate} = \Delta^{15}N \quad (5)$$

However, this internal partitioning is not sufficient to explain the data. The C/N ratios of bulk rocks, which are almost always higher than C/N ratios of bacteria (~7-10, Godfrey and Glass, 2011; Hayes et al., 1983), indicate that a significant amount of nitrogen has been lost from the system. Previous studies have shown that the isotopic effect of metamorphic nitrogen loss is on the order of 1-2‰ up to greenschist facies (reviewed by Thomazo and Papineau, 2013). If we

apply a loss effect of 1‰ to the two phases in our model (Fig. 9B), then the bulk value increases by this amount (dark blue circle), the isotopically light kerogen fraction (green arrow) moves a little bit closer to the unmetamorphosed bulk value (light blue circle) and the isotopically heavy silicate fraction moves further away (brown arrow). Importantly, the isotopic loss effect of 1-2‰ is smaller than $\varepsilon_{internal}$ of 3-4‰ at greenschist facies. Therefore, for samples with relatively low values of $f_{kerogen}$ (< 60%), where $\delta^{15}N_{kerogen}$ would be lightest after applying $\varepsilon_{internal}$ (Fig. 9A, 8B), the final value of $\delta^{15}N_{kerogen}$ after metamorphic loss would still be relatively further removed (lighter) from the initial unaltered bulk value ($\delta^{15}N_{bulk\text{-}initial}$) than the final altered bulk value ($\delta^{15}N_{bulk\text{-}final}$). This scenario is exemplified by the Soanesville samples (Fig. 8C, 7D). Plotting the Soanesville results onto Fig. 9 suggests that these data are best explained by an external loss effect that is intermediate between 0‰ (Fig. 9A, where $\delta^{15}N_{silicate}$ is slightly underestimated by the model) and 1‰ (Fig. 9B, where $\delta^{15}N_{silicate}$ is slightly overestimated). Hence in this case, the measured $\delta^{15}N_{bulk}$ of the metamorphosed sample is a better approximation than $\delta^{15}N_{kerogen}$ for the primary isotopic composition of the biomass. If $f_{kerogen}$ is larger than 60%, then $\delta^{15}N_{kerogen}$ would likely be closer to $\delta^{15}N_{bulk\text{-}initial}$, but our data suggest that this is a rare geological scenario (Fig. 4).

The situation may be different for highly altered samples where the metamorphic loss effect of several permil may be equal to or exceed $\varepsilon_{internal}$. In this case (Fig. 9C), internal partitioning would force $\delta^{15}N_{kerogen}$ light, but this fractionation may be (over-)compensated by metamorphic loss, which raises $\delta^{15}N_{kerogen}$ to values equal or slightly higher than the primary biomass. In such high-grade samples, $\delta^{15}N_{kerogen}$ may thus be a better proxy than $\delta^{15}N_{bulk}$ for reconstructing primary biological metabolisms, because it is not as far removed (Fig. 9C). We only have two data points from the Duffer Formation that may fall into this category. They show elevated values for both $\delta^{15}N_{kerogen}$ (~ +3‰) and $\delta^{15}N_{bulk}$ (~ +13‰) (Fig. 7). Given their Mesoarchean age (3.4 Ga, Wille et al., 2013), the lack of oxygen in the ocean and atmosphere at that time (Lyons et al., 2014), the proposed low seawater pH of 6.5 (Halevy and Bachan, 2017), and $\delta^{15}N_{bulk}$ values around 0‰ from slightly younger but much less metamorphosed rocks (Stüeken et al., 2015a), it is unlikely that the +13‰ bulk values of the Duffer Formation are close to primary. However, $\delta^{15}N_{kerogen}$ values around +3‰ could plausibly reflect the combined effects of internal partitioning (forcing kerogen lighter) and metamorphic loss (forcing it

heavier). The primary isotopic composition of the biomass was that perhaps only slightly lighter than +3‰.

4.4. Implications for the Precambrian nitrogen cycle

The magnitude of these metamorphic effects upon nitrogen partitioning suggests that they may manifest themselves in the older parts of the secular nitrogen isotopic record, as metamorphism tends to be more marked with age. It is notable that in the Precambrian, amphibolite facies $\delta^{15}N$ values are almost always heavier than less metamorphosed age equivalents (Fig. 10) and the same often applies to greenschist-facies values (e.g. Papineau et al., 2009). Our data may thus explain why mica separates from Precambrian sedimentary rocks tend to be isotopically heavier than bulk samples (Jia and Kerrich, 2000; Papineau et al., 2005; Pinti and Hashizume, 2011a), while kerogen isolates in other studies have been found to be isotopically lighter (Ader et al., 2016; Godfrey and Falkowski, 2009; Godfrey et al., 2013; Kump et al., 2011; Stüeken et al., 2015a; Zerkle et al., 2017).

If nitrogen phases separate isotopically with increasing metamorphic grade, then we can use this as a tool to evaluated previously proposed trends in nitrogen isotopes. For example, the unusually high $\delta^{15}N_{bulk}$ values up to +50‰ of the Neoarchean lacustrine Tumbiana Formation (Hayes et al., 1983; Stüeken et al., 2015b; Thomazo et al., 2011) are associated with $\delta^{15}N_{kerogen}$ values that are similar or slightly heavier than bulk samples, which has been attributed to a ppm-level contribution of detrital nitrogen to the very nitrogen-poor sediments (Stüeken et al., 2015b). Large isotopic separations with kerogen becoming lighter than bulk rocks were not observed in any of the samples. The heavy $\delta^{15}N_{bulk}$ values of the Tumbiana Formation are thus most parsimoniously explained by syn-depositional or diagenetic processes, such as aerobic nitrogen cycling (Pinti and Hashizume, 2011b; Thomazo et al., 2011) or NH_3 loss at elevated pH (Stüeken et al., 2015b). High degrees of metamorphic alteration are inconsistent with the trends observed in this study. In contrast, the isotopic enrichments to +11‰ in $\delta^{15}N_{bulk}$ observed by Godfrey et al. (2013) in Paleoproterozoic samples that were taken proximal to a large igneous intrusion have most likely been overprinted by metamorphism, because $\delta^{15}N_{kerogen}$ in the same samples is markedly depleted down to -5‰. Moderate isotopic differences of a few permil between $\delta^{15}N_{bulk}$ and $\delta^{15}N_{kerogen}$ in other Archean and Paleoproterozoic datasets (Godfrey and Falkowski, 2009;

Kump and Arthur, 1999; Zerkle et al., 2017) are consistent with greenschist grade alteration. $\delta^{15}N_{kerogen}$ in these samples may thus have been slightly shifted to lighter values, which however, does not alter the overall conclusions of these particular studies.

5. Conclusion

Our results support several key observations and conclusions for the interpretation of nitrogen isotope data from sedimentary rocks:

- Our data confirm previous observations that a large fraction of sedimentary nitrogen is bound to silicate minerals (Fig. 2) (Godfrey and Falkowski, 2009; Godfrey et al., 2013; Koehler et al., 2017; Kump et al., 2011; Stüeken et al., 2015a; Zerkle et al., 2017), consistent with diagenetic transfer of NH_4^+ from biomass to clays (Müller, 1977; Schroeder and McLain, 1998).
- The relative abundance of the two nitrogen phases does not appear to be a function of metamorphic grade (Fig. 4), most likely because the transfer of NH_4^+ from biomass to clays largely occurs during diagenesis and is controlled by the mineralogy, permeability, and porosity of the sediments (Müller, 1977; Schroeder and McLain, 1998).
- We find a significant isotopic separation between silicate-bound and kerogen-bound nitrogen, where the latter is usually isotopically lighter, consistent with previous studies (Godfrey and Falkowski, 2009; Godfrey et al., 2013; Koehler et al., 2017; Kump et al., 2011; Stüeken et al., 2015a; Zerkle et al., 2017).
- Our data reveal that this isotopic partitioning increases with metamorphic grade (Fig. 3), because kerogen becomes isotopically lighter while silicates becomes heavier (Fig. 8). This observation is most parsimoniously explained by an increase in the equilibrium fractionation factor between the two phases. We speculate that it may be caused by changes in the bonding environments as kerogen thermally matures and phyllosilicates are dewatered with increasing metamorphic grade.
- For rocks up to greenschist facies, the isotopic effect of internal partitioning (3-4‰) is larger than the isotopic effect of metamorphic nitrogen loss (1-2‰) that has been constrained in previous studies (Bauersachs et al., 2009; Bebout et al., 1999; Bebout and

Fogel, 1992; Boyd and Phillippot, 1998; Busigny et al., 2003; Haendel et al., 1986; Jia, 2006; Mingram and Bräuer, 2001; Palya et al., 2011; Pinti et al., 2009; Plessen et al., 2010; Yui, 2009 #758, reviewed by Thomazo and Papineau, 2013). The opposite may be true for samples at higher metamorphic grades (Fig. 9).

In conclusion, for samples up to greenschist facies with more than 40% silicate-bound nitrogen ($f_{kerogen}$ < 60%, which applies to most samples, Fig. 4), the primary isotopic composition of biomass is perhaps best approximated by bulk rock measurements rather than by kerogen isolates. For higher metamorphic grades or rocks with a very large kerogen fraction, on the other hand, kerogen isolates are probably closer to primary biomass, because the effects of internal partitioning and external nitrogen loss offset each other. Isotopic separation between the different nitrogen phases could thus be used as an independent proxy for the degree of metamorphic alteration. We encourage future studies to validate and elucidate these trends.

Acknowledgments

This work was financially supported by a NASA Exobiology grant to RB (# NNX16AI37G), an NSF graduate student research fellowship to JZ, and a NASA postdoctoral fellowship to EES. We thank the Geological Survey of Western Australia for access to the ABDP-2 drill core, Thomas Hearon, Tim Lyons, George & Anne Morphett and Allen & Sharon McInnes for support and hospitality while working on the Callanna Group, and Andy Schauer for technical assistance. We thank Jack Middelburg, Magali Ader and two anonymous reviewers for helpful comments that improved the manuscript.

Table 1: Isotopic and abundance data. References to previously published data are as follows. 1. Nitrogen isotopes, C/N ratios and K abundances for bulk rocks and kerogen isolates taken from Stüeken et al. (2015a); 2. Nitrogen isotopes and C/N ratios of bulk rocks taken from Stüeken (2013); 3. Nitrogen isotopes and C/N ratios of bulk rocks and kerogen isolates taken from Koehler et al. (2017). All other data were collected for this study as described in Section 2. [at] = atomic ratios in mol/mol.

		Bulk rock data					Kerogen data					Silicate data		
ID	Age [Ga]	K [%]	TOC [%]	$\delta^{15}N_{bulk}$ [‰]	TN [%]	C/N_{bulk} [at]	$\delta^{15}N_{kerorgen}$ [‰]	TOC [%]	$C/H_{kerogen}$ [at]	C/N_{ker} [at]	$f_{kerogen}$ [%]	$\delta^{15}N_{silicate}$ [‰]	$\Delta^{15}N$ [‰]	Refs.
Duffer Formation, Australia:														
ABDP2_69	3.4		10.29	13.00	44	2755	3.16	91.0	17.8	14292	16.4	14.93	-11.77	
ABDP2_73	3.4		2.01	12.98	33	714	2.80	93.2	16.7	19440	3.1	13.31	-10.51	
Soanesville Group, Australia:														
96049	3.2	2.11	1.20	0.48	359	39	-1.29	67.4	7.7	285	13.7	0.76	-2.05	1
96050	3.2	1.84	0.76	0.40	348	25	-0.99	51.4	7.8	265	9.6	0.55	-1.53	1
96051	3.2	2.26	1.11	0.42	423	31	-1.63	52.2	6.1	286	10.7	0.67	-2.30	1
96052	3.2	1.77	0.85	0.40	325	30	-1.57	49.1	6.0	251	12.1	0.68	-2.25	1
96053	3.2	1.96	1.23	0.58	405	35	-1.47	57.2	6.9	262	13.5	0.91	-2.38	1
96054	3.2	1.55	1.54	0.14	392	46	-2.08	60.1	6.7	275	16.6	0.59	-2.67	1
96055	3.2	2.25	1.98	0.64	503	46	-1.75	64.2	7.0	281	16.4	1.11	-2.86	1
96056	3.2	1.76	0.96	0.63	360	31	-2.12	53.9	6.8	281	11.1	0.98	-3.10	1
97SSD32-06	3.2	6.18	1.55	0.66	292	62	-1.40	52.2	6.9	297	20.8	1.21	-2.60	1
97SSD32-21	3.2	1.72	1.20	0.37	107	132	-2.24	69.7	7.2	302	43.2	2.36	-4.60	1
97SSD51-03	3.2	1.36	1.42	-0.86	371	45	-2.25	56.7	6.0	267	16.8	-0.58	-1.67	1
Jeerinah Formation, Australia:														
99018	2.65		6.20	-0.45	256	282	0.06	44.59	8.3	607	46.5	1.16	-1.10	
99019	2.65	5.29	4.08	2.37	333	144	-0.02	50.71	8.2	304	47.0	4.49	-4.51	
99021	2.65	5.39	8.17	3.43	730	131	-0.36	49.66	7.8	300	43.6	6.36	-6.72	
99022	2.65	4.63	5.51	3.40	535	120	0.87	42.09	7.3	277	43.7	5.40	-4.53	
Witwatersrand Supergroup, South Africa:														
BAB1-376	2.9	1.56	0.47	3.64	135	41	-0.48	21.3	3.3	394	10.3	4.12	-4.60	1
TF1-4400	2.9	2.31	1.13	-1.17	74	171	-2.28	54.7	9.8	1910	9.3	-1.06	-1.23	1
TF1-4440	2.9	3.58	0.78	-1.33	106	86	-4.44	67.5	14.6	1781	4.8	-1.18	-3.27	1
TW6-1749.9	2.9	1.37	0.33	0.57	39	102	-2.17	16.6	5.7	1279	7.7	0.80	-2.98	1
TW6-1750.2	2.9	1.88	0.56	1.53	64	104	-1.79	27.6	6.3	1251	8.3	1.83	-3.62	1
Nullagine Group, Australia:														

130711-4	2.9	2.59	0.23	0.06	42	64	-0.17	38.87	5.7	375	17.3	0.11	-0.27	1
Bangemall Group, Australia:														
89028	1.5		0.35	0.95	48	85	1.27	43.2	2.9	97	86.4	-1.05	2.32	
Belt Supergroup, USA:														
110715-7	1.45		0.58	5.02	422	16	5.65	56.7	3.2	124	13.0	4.93	0.73	2
110719-4	1.45		0.43	4.90	490	10	4.40	55.6	3.1	106	9.7	4.96	-0.56	2
110720-1	1.45		0.65	1.52	251	30	3.19	40.4	2.2	108	28.1	0.86	2.33	2
110722-19	1.45		0.32	0.60	433	9	-1.67	27.5	2.8	229	3.8	0.69	-2.36	2
110722-20	1.45		0.15	-0.40	201	9	1.91	13.5	2.9	106	8.2	-0.60	2.52	2
110722-22	1.45		0.21	0.49	315	8	0.02	6.9	2.3	165	4.8	0.51	-0.50	2
110723-3	1.45		0.50	-0.82	181	32	-1.11	62.1	4.3	164	19.8	-0.75	-0.36	2
110723-6	1.45		0.31	-0.95	315	12	-1.40	24.6	3.9	133	8.7	-0.91	-0.49	2
120701-11	1.45		1.10	5.00	439	29	4.72	69.7	3.4	119	24.6	5.09	-0.37	2
Roper Group, Australia:														
A8231_391.0	1.4		0.50	4.61	311	19	4.57	40.8	1.5	80	23.5	4.62	-0.05	3
BR1_23.4	1.4		0.08	2.11	429	2	2.55	16.3	1.1	90	2.4	2.10	0.46	3
BR1_244.7	1.4		0.09	3.66	227	5	2.63	15.6	1.6	110	4.3	3.71	-1.07	3
GG1_53.2	1.4		0.24	1.39	326	8	2.86	34.0	0.8	47	18.1	1.07	1.79	3
U4_33.2	1.4		0.40	4.76	116	41	5.34	23.2	1.3	61	66.3	3.63	1.72	3
U4_82.25	1.4		0.51	2.95	375	16	3.55	35.7	1.0	68	23.2	2.77	0.79	3
Callanna Group, Australia:														
150828-8	0.8		2.11	5.92	88	278	4.23	76.9	15.6	642	43.2	7.25	-3.02	
150828-15	0.8	3.1	0.93	4.59	167	65	1.98	61.7	12.3	622	11.1	4.93	-2.95	
150828-22	0.8	3.2	0.30	3.80	145	24	1.06	53.7	11.4	832	2.7	3.88	-2.82	
150907-3	0.8	4.37	0.24	4.15	311	9	0.39	26.75	7.5	227	4.0	4.31	-3.92	
150907-15	0.8	4.71	0.24	4.20	323	9	0.45	61.7	5.7	227	3.8	4.35	-3.90	
150907-29	0.8	4.18	0.26	4.73	380	8	0.89	38.30	7.1	217	3.8	4.88	-3.99	
150908-2	0.8	6.84	0.36	4.94	186	22	0.73	25.3	4.5	223	9.7	5.41	-4.68	
150908-14	0.8	4.97	0.29	4.63	166	20	0.86	33.03	7.9	220	8.9	5.00	-4.15	
Sulphur Mountain Formation, Canada:														
OCB +10	0.25		0.04	3.49	118	4	6.18	1.19	1.1	26	14.3	3.05	3.14	
OCB +2.5	0.25		0.04	3.45	128	4	7.42	0.68	1.0	21	19.8	2.47	4.95	
OCB +22	0.25		0.51	3.30	316	19	2.92	5.59	1.7	43	44.7	3.61	-0.69	

Figure captions

Figure 1: Nitrogen isotopes in different phases of selected samples through time. Shown are only those samples that were analyzed in this study. To reconstruct environmental trends, it needs to be resolved which post-metamorphic phase is closest to original biomass.

Figure 2: Molar ratios of organic carbon to organic hydrogen versus molar ratios of organic carbon to organic nitrogen (kerogen) or total nitrogen (bulk). Molar C/H ratios are a widely-accepted proxy for metamorphic alteration, because H is lost preferentially over C. The correlation shows that C/H ratios also track metamorphic N loss and can thus be used as a measure for metamorphic alteration of nitrogen isotopes. Bulk rocks have lower C/N ratios than kerogen extracts, because they contain additional silicate-bound nitrogen. C/H ratios are matched with metamorphic facies following the calibration by Hayes et al. (1983).

Figure 3: Molar C/H ratios of kerogen versus δ^{15}N difference between kerogen and silicate-bound nitrogen. The silicate-bound phase was calculated by mass balance from the measured kerogen and bulk rock values. Anti-correlation shows that the two nitrogen phases diverge isotopically with increasing metamorphic grade (higher C/H ratio). C/H ratios are matched with metamorphic facies following the calibration by Hayes et al. (1983). If the two high-grade negative extremes in Δ^{15}N are removed, the correlation coefficient is 0.53.

Figure 4: (A) Molar C/H ratio versus the fraction of kerogen-bound nitrogen $f_{kerogen}$, and (B) the $f_{kerogen}$ versus the isotopic difference Δ^{15}N between kerogen and silicates. The lack of a correlation in both plots suggest that $f_{kerogen}$ is not to first order controlled by metamorphism, and that the isotopic difference between phases is independent from the abundance distribution. Instead it implies that the fractionation factor between kerogen and silicate-bound N changes with metamorphic grade.

Figure 5: Bulk rock K abundances versus N-isotopic difference Δ^{15}N between phases. The lack of a correlation argues against a significant metasomatic effect on the fractionation factor between N-bearing phases. Instead it is more likely that the fractionation factor changes as a function of bond strengths or bonding environment as clay minerals turn into micas and biomass becomes increasingly mature. This may be different for the Callanna samples, which show a moderate correlation with K and may have been affected by metasomatism. But more samples from clearly metasomatised settings are needed to address this question.

Figure 6: Kerogen carbon content versus Δ^{15}N. The kerogen isolates are not composed of pure carbon (TOC < 100%), likely due to dilution by recalcitrant minerals that are poorly soluble in HF at 50°C. However, the lack of correlation between kerogen TOC and Δ^{15}N indicates that the impurity of the kerogen isolates does not affect the trends in our data. The dashed grey trend line includes all data points, the solid black trend line excludes the four most extreme data points that are marked in grey.

Figure 7: Isotopic difference $\Delta^{15}N$ between nitrogen phases versus raw isotopic value of each phase. Both phases show a high degree of variability, which could be due to metamorphic effects but also primary biological nitrogen isotope fractionation in the environment. Isolating the metamorphic effect requires focusing on samples from the N_2-fixation range (-2‰ to +1‰).

Figure 8: Nitrogen isotopes of different phases in samples from the N_2-fixation range. A: all samples, B: Belt Supergroup (1.5 Ga), C: Soanesville Group (3.2 Ga) all samples, D: Soanesville Group data with an outlier at $\Delta^{15}N$ = 4.6‰ removed. Inverse slopes show that both phases change their isotopic composition: kerogen-bound N gets lighter as silicate-bound N gets heavier. Silicates are slightly more affected than kerogen.

Figure 9: Equilibrium fractionation model. During diagenesis, biomass-bound N partitions partly into clay minerals up to a certain value of $f_{kerogen}$ that likely depends on the mineralogy of the host rock. With increasing metamorphic grade, the two N phases (kerogen and silicate) separate isotopically, probably without a significant effect on $f_{kerogen}$ (Fig. 4B). The higher the metamorphic grade, the larger the fractionation $\varepsilon_{internal}$ between kerogen and silicate-N (gray fans in panel A, with $\varepsilon_{internal}$ ranging from 1‰ to 4‰). At high $f_{kerogen}$, as observed in the Soanesville samples, $\delta^{15}N_{kerogen}$ would be significantly lighter than $\delta^{15}N_{bulk\text{-}initial}$ while $\delta^{15}N_{silicate}$ would only be slightly heavier. Without loss of nitrogen from the system (panel A), $\delta^{15}N_{bulk\text{-}initial}$ would be equal to the original biomass. If nitrogen is lost from the system (from both phases) with a small isotopic effect (here 1‰ as in sub-greenschist facies), then the measured bulk value becomes slightly heavier ($\delta^{15}N_{bulk\text{-}final}$ = +1‰, panel B), but at high $f_{kerogen}$ and high $\varepsilon_{internal}$, $\delta^{15}N_{bulk\text{-}final}$ is still closer to $\delta^{15}N_{bulk\text{-}initial}$ than $\delta^{15}N_{kerogen}$. This scenario matches the observation from the Soanesville samples (Fig. 5C, 5D). If nitrogen is lost with a large isotopic effect (here 5‰ as in upper-greenschist facies or above, panel C), then the final $\delta^{15}N_{kerogen}$ is closer to $\delta^{15}N_{bulk\text{-}initial}$ than $\delta^{15}N_{bulk\text{-}final}$. In such cases, kerogen is the better proxy for primary biomass. This scenario may be exemplified by the Duffer samples that show the highest metamorphic grade in our sample set (Fig. 7).

Figure 10: Secular record of nitrogen isotopes segregated by metamorphic grade. Data are compiled from several references (database available from Stüeken et al., 2016). The compilation shows that rocks of higher metamorphic grades generally have heavier $\delta^{15}N$ values than lower-grade equivalents. The lacustrine carbonates at 2.72 Ga likely represent an unusual nitrogen cycle in an alkaline lake that favored N-loss as NH_3 (Stüeken et al., 2015b).

References

Ader, M., Cartigny, P., Boudou, J.-P., Oh, J.-H., Petit, E. and Javoy, M., 2006. Nitrogen isotopic evolution of carbonaceous matter during metamorphism: methodology and preliminary results. Chemical Geology, 232: 152-169.

Ader, M., Sansjofre, P., Halverson, G.P., Busigny, V., Trindade, R.I., Kunzmann, M. and Nogueira, A.C., 2014. Ocean redox structure across the Late Neoproterozoic oxygenation event: A nitrogen isotope perspective. Earth and Planetary Science Letters, 396: 1-13.

Ader, M., Thomazo, C., Sansjofre, P., Busigny, V., Papineau, D., Laffont, R., Cartigny, P. and Halverson, G.P., 2016. Interpretation of the nitrogen isotopic composition of Precambrian sedimentary rocks: Assumptions and perspectives. Chemical Geology, 429: 93-110.

Algeo, T.J., Meyers, P.A., Robinson, R.S., Rowe, H. and Jiang, G.Q., 2014. Icehouse-greenhouse variations in marine denitrification. Biogeosciences, 11(4): 1273-1295.

Altabet, M.A., Deuser, W.G., Honjo, S. and Stienen, C., 1991. Seasonal and depth-related changes in the source of sinking particles in the North Atlantic. Nature, 354: 136-139.

Bauersachs, T., Kremer, B., Schouten, S. and Sinninghe Damsté, J.S., 2009. A biomarker and $\delta^{15}N$ study of thermally altered Silurian cyanobacterial mats. Organic Geochemistry, 40(2): 149-157.

Beaumont, V. and Robert, F., 1999. Nitrogen isotope ratios of kerogens in Precambrian cherts: a record of the evolution of atmosphere chemistry? Precambrian Research, 96: 63-82.

Beaumont, V.I., Jahnke, L.L. and Des Marais, D.J., 2000. Nitrogen isotopic fractionation in the synthesis of photosynthetic pigments in *Rhodobacter capsulatus* and *Anabaena cylindrica*. Organic Geochemistry, 31(11): 1075-1085.

Bebout, G.E., Cooper, D.C., Bradley, A.D. and Sadofsky, S.J., 1999. Nitrogen-isotope record of fluid-rock interactions in the Skiddaw Aureole and granite, English Lake District. American Mineralogist, 84: 1495-1505.

Bebout, G.E. and Fogel, M.L., 1992. Nitrogen-isotopic composition of metasedimentary rocks in the Catalina Schist, California: implications for metamorphic devolatilization history. Geochimica et Cosmochimica Acta, 56: 2839-2849.

Boudou, J.P., Schimmelmann, A., Ader, M., Mastalerz, M., Sebilo, M. and Gengembre, L., 2008. Organic nitrogen chemistry during low-grade metamorphism. Geochimica et Cosmochimica Acta, 72(4): 1199-1221.

Boudreau, B.P. and Canfield, D.E., 1988. A provisional diagenetic model for pH in anoxic porewaters: Application to the FOAM site. Journal of Marine Research, 46(2): 429-455.

Boyd, S.R. and Phillippot, P., 1998. Precambrian ammonium biogeochemistry: a study of the Moine metasediments, Scotland. Chemical Geology, 144: 257-268.

Busigny, V., Cartigny, P. and Philippot, P., 2011. Nitrogen isotopes in ophiolitic metagabbros: A re-evaluation of modern nitrogen fluxes in subduction zones and implication for the early Earth atmosphere. Geochimica et Cosmochimica Acta, 75(23): 7502–7521.

Busigny, V., Cartigny, P., Philippot, P., Ader, M. and Javoy, M., 2003. Massive recycling of nitrogen and other fluid-mobile elements (K, Rb, Cs, H) in a cold slab environment: evidence from HP to UHP oceanic metasediments of the Schistes Lustrés nappe (western Alps, Europe). Earth and Planetary Science Letters, 215(1): 27-42.

Busigny, V., Lebeau, O., Ader, M., Krapež, B. and Bekker, A., 2013. Nitrogen cycle in the Late Archean ferruginous ocean. Chemical Geology, 362: 115-130.

Chicarelli, M.I., Hayes, J.M., Popp, B.N., Eckardt, C.B. and Maxwell, J.R., 1993. Carbon and nitrogen isotopic compositions of alkyl porphyrins from the Triassic Serpiano oil shale. Geochimica et Cosmochimica Acta, 57: 1307-1311.

Coplen, T.B., Brand, W.A., Gehre, M., Gröning, M., Meijer, H.A., Toman, B. and Verkouteren, R.M., 2006. New guidelines for $\delta^{13}C$ measurements. Analytical Chemistry, 78(7): 2439-2441.

Durand, B. and Nicaise, G., 1980. Procedures for kerogen isolation. In: B. Durand (Editor), Kerogen. Editions Technip, Paris, pp. 35-53.

Eigenbrode, J.L. and Freeman, K.H., 2006. Late Archean rise of aerobic microbial ecosystems. Proceedings of the National Academy of Sciences, 103(43): 15759-15764.

French, K.L., Hallmann, C., Hope, J.M., Schoon, P.L., Zumberge, J.A., Hoshino, Y., Peters, C.A., George, S.C., Love, G.D., Brocks, J.J. and Buick, R., 2015. Reappraisal of hydrocarbon biomarkers in Archean rocks. Proceedings of the National Academy of Sciences, 112(9): 5915-5920.

Garvin, J., Buick, R., Anbar, A.D., Arnold, G.L. and Kaufman, A.J., 2009. Isotopic evidence for an aerobic nitrogen cycle in the latest Archean. Science, 323: 1045-1048.

Godfrey, L.V. and Falkowski, P.G., 2009. The cycling and redox state of nitrogen in the Archaean ocean. Nature Geoscience, 2: 725-729.

Godfrey, L.V. and Glass, J.B., 2011. The geochemical record of the ancient nitrogen cycle, nitrogen isotopes, and metal cofactors. Methods in Enzymology, 486: 483-506.

Godfrey, L.V., Poulton, S.W., Bebout, G.E. and Fralick, P.W., 2013. Stability of the nitrogen cycle during development of sulfidic water in the redox-stratified late Paleoproterozoic ocean. Geology, 41(6): 655-658.

Haendel, D., Muehle, K., Nitzsche, H.-M., Stiehl, G. and Wand, U., 1986. Isotopic variations of the fixed nitrogen in metamorphic rocks. Geochimica et Cosmochimica Acta, 50: 749-758.

Halevy, I. and Bachan, A., 2017. The geologic history of seawater pH. Science, 355: 1069-1071.

Han, W., Feng, L., Li, H. and Liu, W., 2017. Bulk $\delta^{15}N$ measurements of organic- rich rock samples by elemental analyzer/isotope ratio mass spectrometry with enhanced oxidation ability. Rapid Communications in Mass Spectrometry, 31(1): 16-20.

Hayes, J.M., Kaplan, I.R. and Wedeking, K.W., 1983. Precambrian organic geochmistry, preservation of the record. In: J.W. Schopf (Editor), Earth's earliest biosphere - its origin and evolution. Princeton University Press, Princeton, NJ, pp. 93-134.

Hedges, J.I. and Keil, R.G., 1995. Sedimentary organic matter preservation: an assessment and speculative synthesis. Marine Chemistry, 49(2): 81-115.

Honma, H. and Itihara, Y., 1981. Distribution of ammonium in minerals of metamorphic and granitic rocks. Geochimica et Cosmochimica Acta, 45(6): 983-988.

Hoops, G.K., 1964. The nature of the insoluble residues remaining after the HF-H_2SO_4 acid decomposition (solution B) of rocks. Geochimica et Cosmochimica Acta, 28(3): 405-406.

Itihara, Y. and Honma, H., 1979. Ammonium in biotite from metamorphic and granitic rocks of Japan. Geochimica et Cosmochimica Acta, 43(4): 503-509.

Jackson, M.J., Sweet, I.P. and Powell, T.G., 1988. Studies on Petroleum geology and geochemistry, Middle Proterozoic, McArthur Basin, northern Australia: I. Petroleum potential. APEA J, 28(1): 283-302.

Jia, Y., 2006. Nitrogen isotope fractionations during progressive metamorphism: a case study from the Paleozoic Cooma metasedimentary complex, southeastern Australia. Geochimica et Cosmochimica Acta, 70: 5201-5214.

Jia, Y. and Kerrich, R., 2000. Giant quartz vein systems in accretionary orogenic belts: the evidence for a metamorphic fluid origin from $\delta^{15}N$ and $\delta^{13}C$ studies. Earth and Planetary Science Letters, 184(1): 211-224.

Kashiyama, Y., Ogawa, N.O., Kuroda, J., Shiro, M., Nomoto, S., Tada, R., Kitazato, H. and Ohkouchi, N., 2008. Diazotrophic cyanobacteria as the major photoautotrophs during mid-Cretaceous oceanic anoxic events: Nitrogen and carbon isotopic evidence from sedimentary porphyrin. Organic Geochemistry, 39(5): 532-549.

Kirsten, W.J. and Hesselius, G.U., 1983. Rapid, automatic, high capacity Dumas determination of nitrogen. Microchemical Journal, 28(4): 529-547.

Koehler, M.C., Stüeken, E.E., Kipp, M.A., Buick, R. and Knoll, A.H., 2017. Spatial and temporal trends in Precambrian nitrogen cycling: a Mesoproterozoic offshore nitrate minimum. Geochimica et Cosmochimica Acta, 198: 315-337.

Kump, L.R. and Arthur, M.A., 1999. Interpreting carbon-isotope excursions: carbonates and organic matter. Chemical Geology, 161(1): 181-198.

Kump, L.R., Junium, C., Arthur, M.A., Brasier, A., Fallick, A., Melezhik, V., Lepland, A., CČrne, A.E. and Luo, G., 2011. Isotopic evidence for massive oxidation of organic matter following the Great Oxidation Event. Science, 334(6063): 1694-1696.

Lyons, T.W., Reinhard, C.T. and Planavsky, N.J., 2014. The rise of oxygen in Earth's early ocean and atmosphere. Nature, 506: 307-315.

Macko, S.A., Fogel, M.L., Hare, P.E. and Hoering, T.C., 1987. Isotopic fractionation of nitrogen and carbon in the synthesis of amino acids by microorganisms. Chemical Geology, 65(1): 79-92.

Mariotti, A., 1983. Atmospheric nitrogen is a reliable standard for natural ^{15}N abundance measurements. Nature, 303: 685-687.

Mingram, B. and Bräuer, K., 2001. Ammonium concentration and nitrogen isotope composition in metasedimentary rocks from different tectonometamorphic units of the European Variscan Belt. Geochimica et Cosmochimica Acta, 65(2): 273-287.

Müller, P.J., 1977. CN ratios in Pacific deep-sea sediments: Effect of inorganic ammonium and organic nitrogen compounds sorbed by clays. Geochimica et Cosmochimica Acta, 41(6): 765-776.

Palya, A.P., Buick, I.S. and Bebout, G.E., 2011. Storage and mobility of nitrogen in the continental crust: Evidence from partially melted metasedimentary rocks, Mt. Stafford, Australia. Chemical Geology, 281(3): 211-226.

Papineau, D., Mojzsis, S.J., Karhu, J.A. and Marty, B., 2005. Nitrogen isotopic composition of ammoniated phyllosilicates: case studies from Precambrian metamorphosed sedimentary rocks. Chemical Geology, 216(1): 37-58.

Papineau, D., Purohit, R., Goldberg, T., Pi, D., Shields, G.A., Bhu, H., Steele, A. and Fogel, M.L., 2009. High primary productivity and nitrogen cycling after the Paleoproterozoic phosphogenic event in the Aravalli Supergroup, India. Precambrian Research, 171: 37-56.

Pinti, D.L. and Hashizume, K., 2001. 15N-depleted nitrogen in early Archean kerogens: clues on ancient marine chemosynthetic-based ecosystems? A comment to Beaumont, V. Robert, F. 1999. Precambrian Res. 96, 52-82. Precambrian Research, 105: 85-88.

Pinti, D.L. and Hashizume, K., 2011a. Can the evolution of nitrogen cycle be traced by the N isotopic composition in mica?, AGU, San Francisco, pp. 218.

Pinti, D.L. and Hashizume, K., 2011b. Early life record from nitrogen isotopes. In: S.D. Golding and M. Glikson (Editors), Earliest life on Earth: habitats, environments and methods of detection. Springer, Netehrlands, pp. 183-205.

Pinti, D.L., Hashizume, K. and Matsuda, J.I., 2001. Nitrogen and argon signatures in 3.8 to 2.8 Ga metasediments: Clues on the chemical state of the Archean ocean and the deep biosphere. Geochimica et Cosmochimica Acta, 65(14): 2301-2315.

Pinti, D.L., Hashizume, K., Sugihara, A., Massault, M. and Philippot, P., 2009. Isotopic fractionation of nitrogen and carbon in Paleoarchean cherts from Pilbara craton, Western Australia: Origin of 15N-depleted nitrogen. Geochimica et Cosmochimica Acta, 2009: 3819-3848.

Plessen, B., Harlov, D.E., Henry, D. and Guidotti, C.V., 2010. Ammonium loss and nitrogen isotopic fractionation in biotite as a function of metamorphic grade in metapelites from western Maine, USA. Geochimica et Cosmochimica Acta, 74: 4759-4771.

Preiss, W., 1987. The Adelaide Geosyncline: Late Proterozoic stratigraphy, sedimentation, palaeontology and tectonics, 53. Department of Mines and Energy, Adelaide, Australia.

Robl, T.L. and Davis, B.H., 1993. Comparison of the HF-HCl and HF-BF_3 maceration techniques and the chemistry of resultant organic concentrates. Organic Geochemistry, 20(2): 249-255.

Rosenfeld, J.K., 1979. Ammonium adsorption in nearshore anoxic sediments. Limnology and Oceanography, 24(2): 356-364.

Schieber, J., 1989. Facies and origin of shales from the mid-Proterozoic Newland Formation, Belt basin, Montana, USA. Sedimentology, 36: 203-219.

Schimmelmann, A. and Lis, G.P., 2010. Nitrogen isotopic exchange during maturation of organic matter. Organic Geochemistry, 41(1): 63-70.

Schimmelmann, A., Mastalerz, M., Gao, L., Sauer, P.E. and Topalov, K., 2009. Dike intrusions into bituminous coal, Illinois Basin: H, C, N, O isotopic responses to rapid and brief heating. Geochimica et Cosmochimica Acta, 73(20): 6264-6281.

Schoepfer, S.D., Henderson, C.M., Garrison, G.H., Foriel, J., Ward, P.D., Selby, D., Hower, J.C., Algeo, T.J. and Shen, Y., 2013. Termination of a continent-margin upwelling system at the Permian–Triassic boundary (Opal Creek, Alberta, Canada). Global and Planetary Change, 105: 21-35.

Schoepfer, S.D., Henderson, C.M., Garrison, G.H. and Ward, P.D., 2012. Cessation of a productive coastal upwelling system in the Panthalassic Ocean at the Permian–Triassic Boundary. Palaeogeography, Palaeoclimatology, Palaeoecology, 313-314: 181-188.

Schroeder, P.A. and McLain, A.A., 1998. Illite-smectites and the influence of burial diagenesis on the geochemical cycling of nitrogen. Clay Minerals, 33(4): 539-546.

Stüeken, E.E., 2013. A test of the nitrogen-limitation hypothesis for retarded eukaryote radiation: nitrogen isotopes across a Mesoproterozoic basinal profile. Geochimica et Cosmochimica Acta, 120: 121-139.

Stüeken, E.E., Buick, R., Guy, B.M. and Koehler, M.C., 2015a. Isotopic evidence for biological nitrogen fixation by Mo-nitrogenase at 3.2 Gyr. Nature, 520: 666-669.

Stüeken, E.E., Buick, R. and Schauer, A.J., 2015b. Nitrogen isotope evidence for alkaline lakes on late Archean continents. Earth and Planetary Science Letters, 411: 1-10.

Stüeken, E.E., Foriel, J., Buick, R. and Schoepfer, S.D., 2015c. Selenium isotope ratios, redox changes and biological productivity across the end-Permian mass extinction. Chemical Geology, 410: 28-39.

Stüeken, E.E., Kipp, M.A., Koehler, M.C. and Buick, R., 2016. The evolution of Earth's biogeochemical nitrogen cycle. Earth Science Reviews, 160: 220-239.

Svensen, H., Bebout, G., Kronz, A., Li, L., Planke, S., Chevallier, L. and Jamtveit, B., 2008. Nitrogen gechemistry as a tracer of fluid flow in a hydrothermal vent complex in the Karoo Basin, South Africa. Geochimica et Cosmochimica Acta, 72: 4929-4947.

Talbot, M.R. and Johannessen, T., 1992. A high resolution palaeoclimatic record for the last 27,500 years in tropical west Africa from the carbon and nitroen isotopic composition of lacustrine organic matter. Earth and Planetary Science Letters, 110: 23-37.

Therion, J.J., Human, H.G.C., Claase, C., Mackie, R.I. and Kistner, A., 1986. Automatic nitrogen-15 analyser for use in biological research. Analyst, 111: 1017-1021.

Thomazo, C., Ader, M. and Phillippot, P., 2011. Extreme ^{15}N-enrichment in 2.72-Gyr-old sediments: evidence for a turning point in the nitrogen cycle. Geobiology, 9: 107-120.

Thomazo, C. and Papineau, D., 2013. Biogeochemical cycling of nitrogen on the early Earth. Elements, 9(5): 345-351.

Thomazo, C., Pinti, D.L., Busigny, V., Ader, M., Hashizume, K. and Phillippot, P., 2009. Biological activity and the Earth's surface evolution: insights from carbon, sulfur, nitrogen and iron stable isotopes in the rock record. C. R. Palevol, 8: 665-678.

van de Kamp, P.C., 2016. Potassium distribution and metasomatism in pelites and schists: how and when, relation to postdepositional events. Journal of Sedimentary Research, 86: 683-711.

Van Krevelen, D.W., 1950. Graphical-statistical method for the study of structure and reaction processes of coal. Fuel, 29: 269-283.

Van Krevelen, D.W., 1984. Organic geochemistry-old and new. Organic Geochemistry, 6: 1-10.

van Zuilen, M.A., Mathew, K., Wopenka, B., Lepland, A., Marti, K. and Arrhenius, G., 2005. Nitrogen and argon isotopic signatures in graphite from the 3.8-Ga-old Isua Supracrustal Belt, Southern West Greenland. Geochimica et Cosmochimica Acta, 69(5): 1241-1252.

Wille, M., Nebel, O., Van Kranendonk, M.J., Schoenberg, R., Kleinhanns, I.C. and Ellwood, M.J., 2013. Mo-Cr-isotope evidence or a reducing Archean atmosphere in 3.46-2.76 Ga black shales from the Pilbara, Western Australia. Chemical Geology, 340: 68-76.

Yamaguchi, K.E., 2002. Geochemistry of Archean-Paleoproterozoic black shales: the early evolution of the atmosphere, oceans, and biosphere. PhD dissertation Thesis, Pennsylvania State University, 485 pp.

Yui, T.-F., Kao, S.-J. and Wu, T.-W., 2009. Nitrogen and N-isotope variation during low-grade metamorphism of the Taiwan mountain belt. Geochemical Journal, 43: 15-27.

Zerkle, A.L., Poulton, S.W., Newton, R.J., Mettam, C., Claire, M.W., Bekker, A. and Junium, C.K., 2017. Onset of the aerobic nitrogen cycle during the Great Oxidation Event. Nature, 542: 465-467.

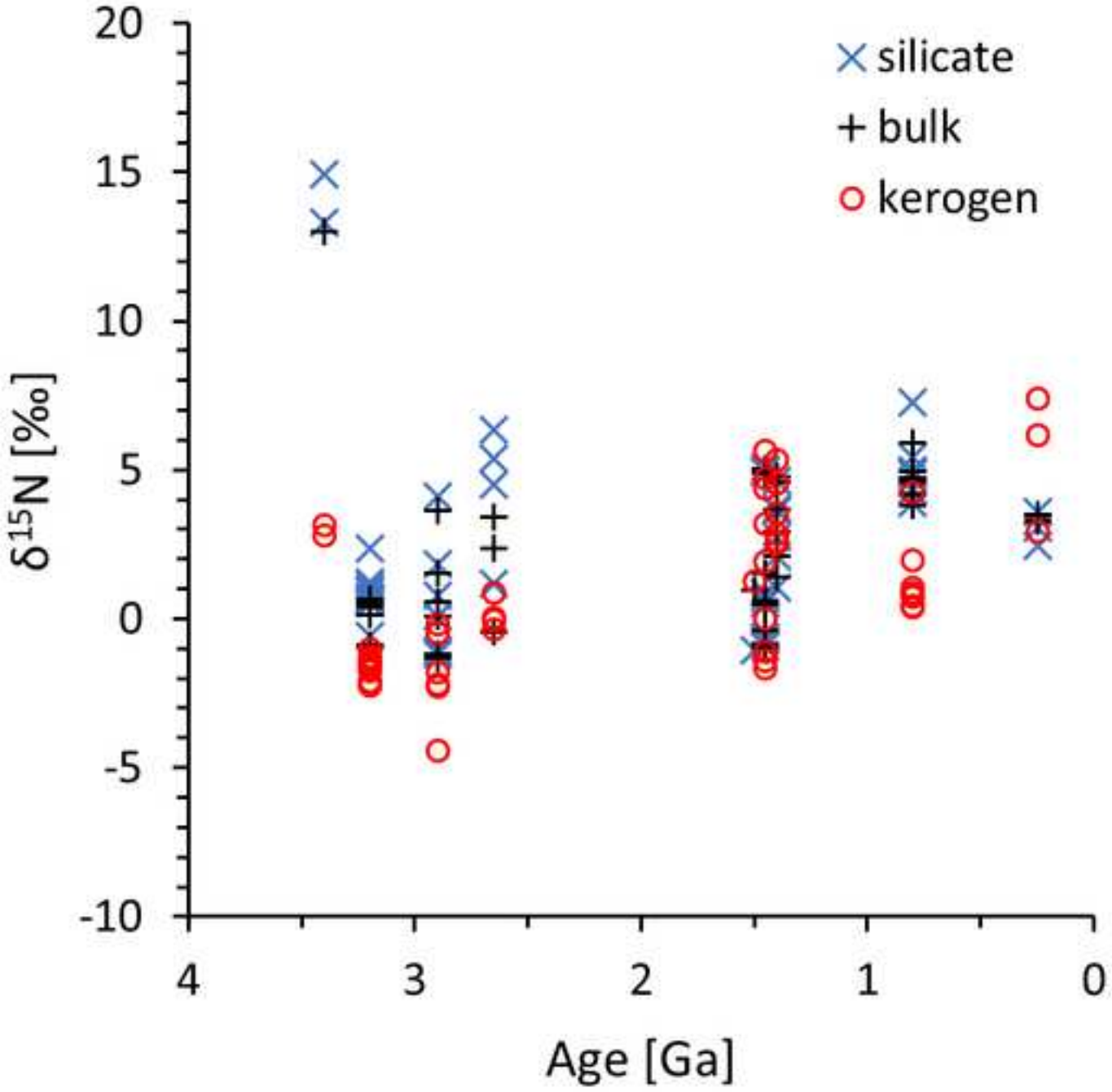
silicate
bulk
kerogen
δ15N [‰]
20
15
10
5
0
-5
-10
4
3
2
1
0
Age [Ga]

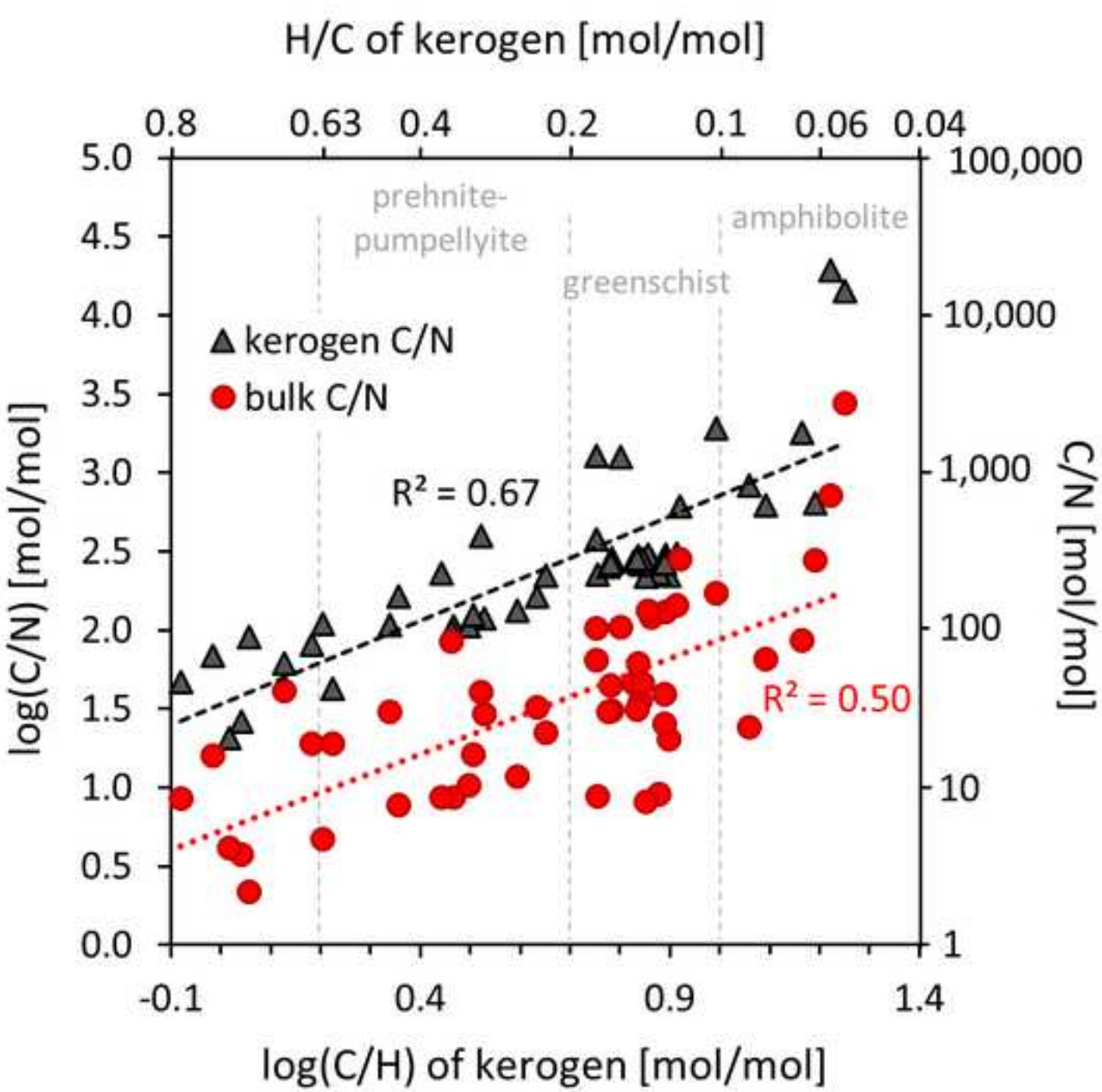

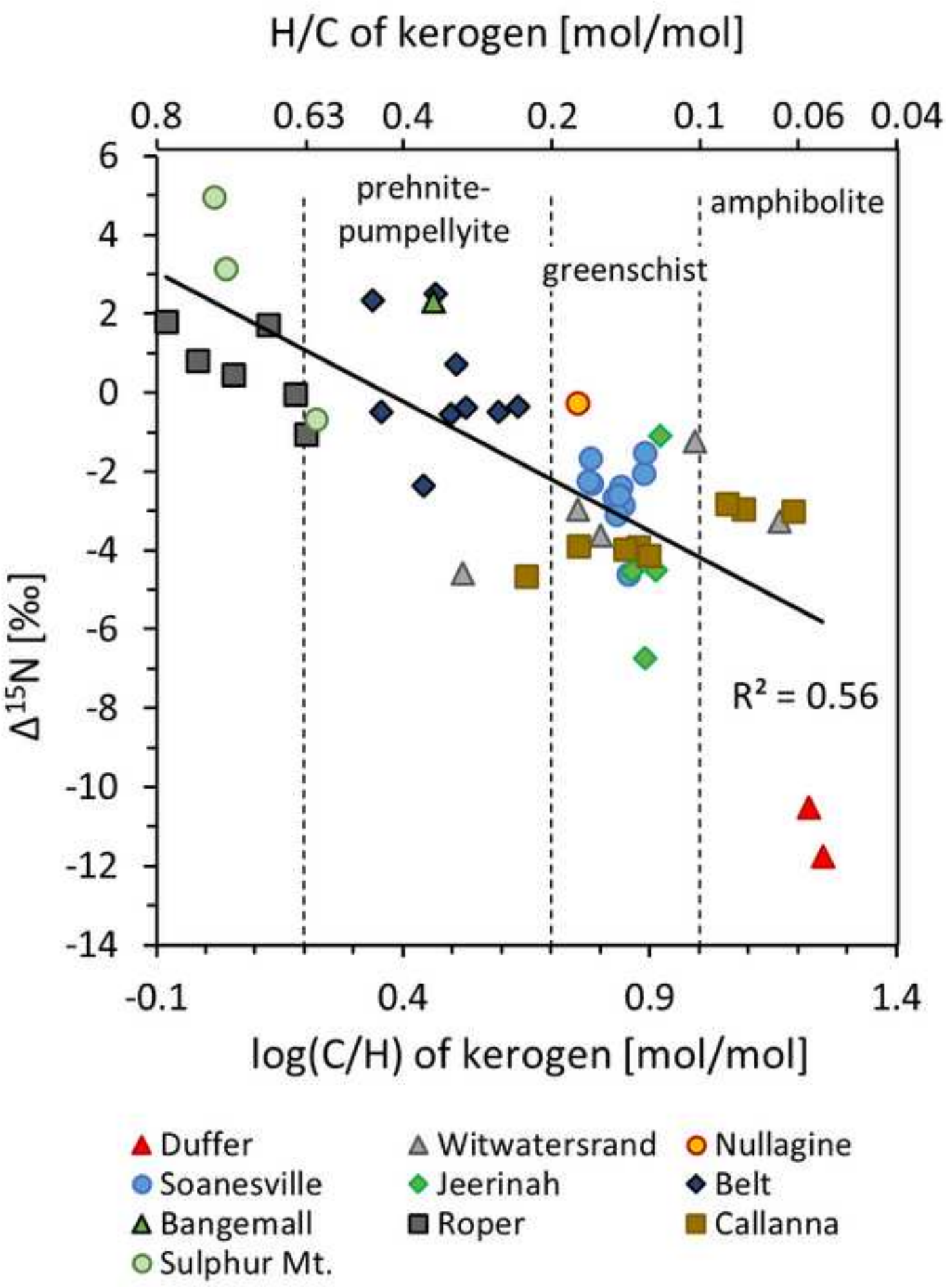

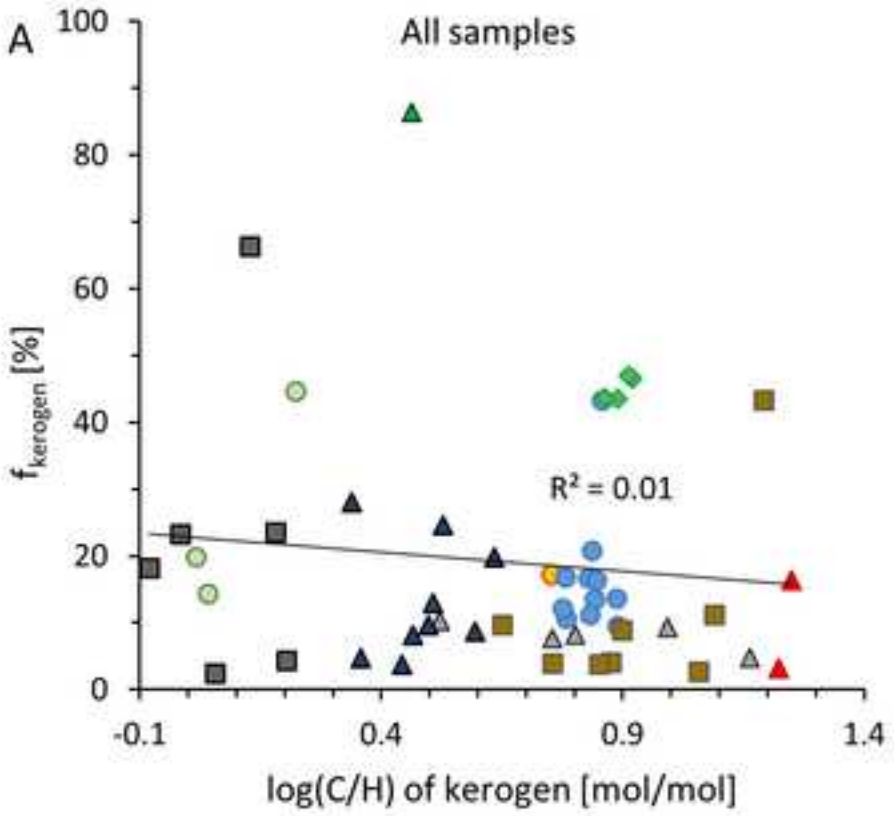

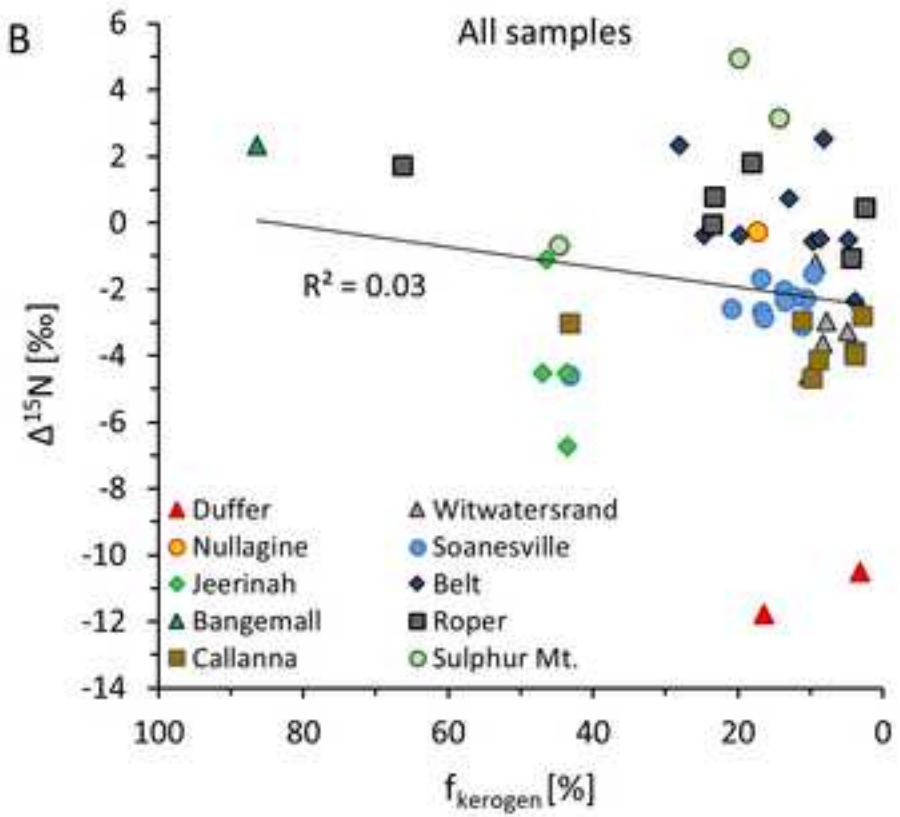

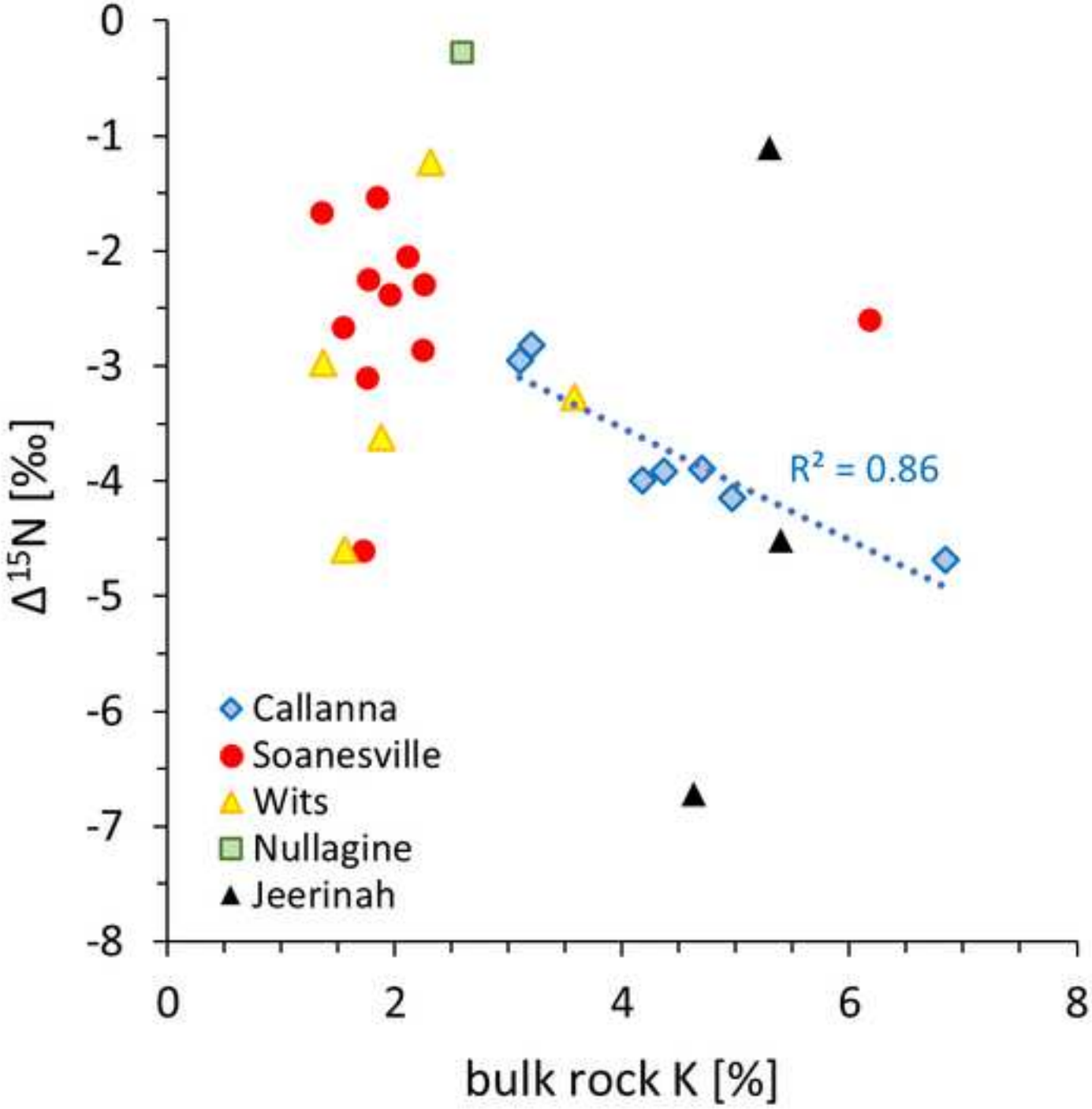

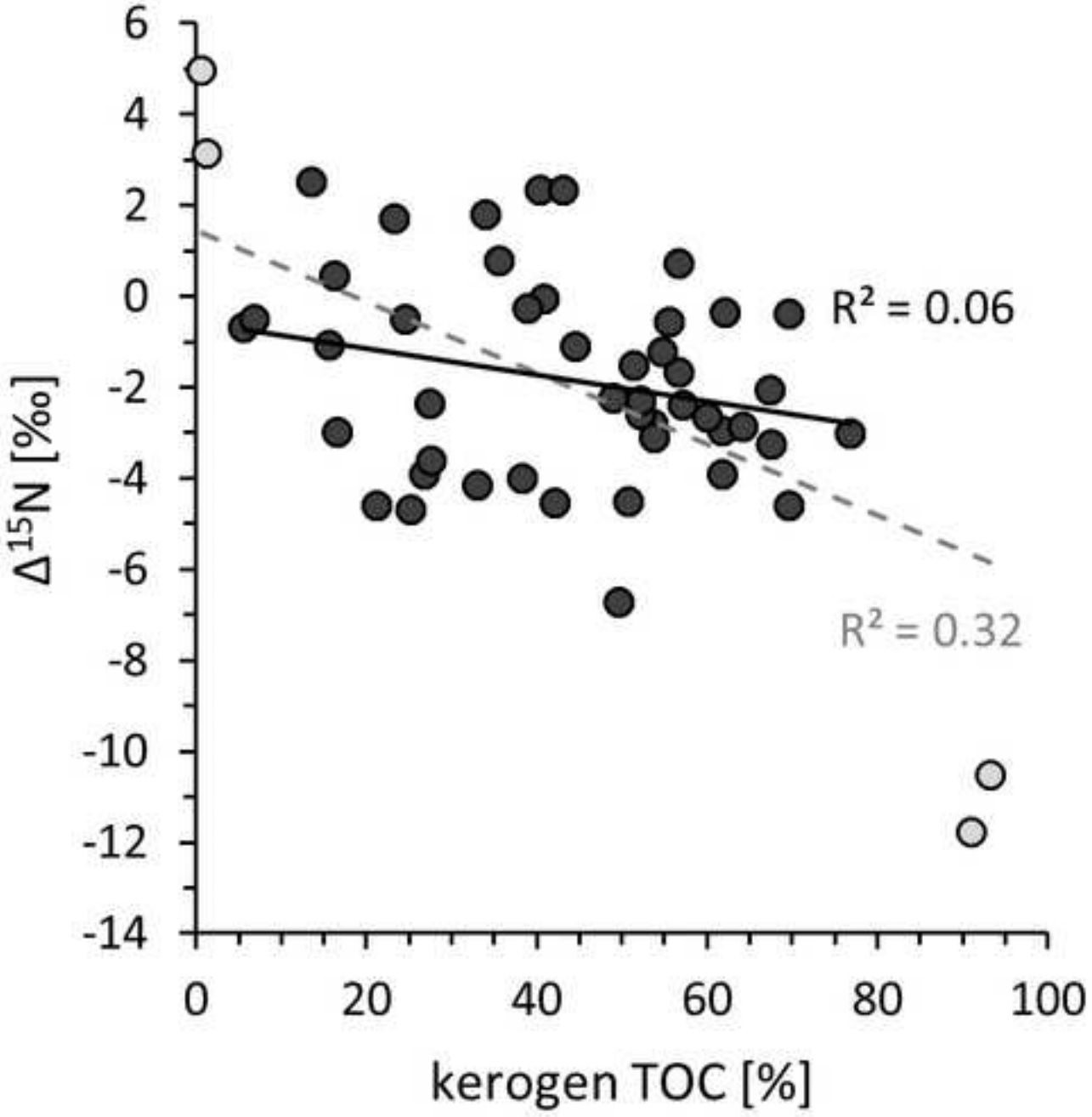
6
4
2
0
-2
-4
-6
-8
-10
-12
-14
Δ15N [‰]
0
20
40
60
80
100
kerogen TOC [%]
R² = 0.06
R² = 0.32